Published in final edited form as:
J Am Chem Soc. 2013 August 14; 135(32): . doi:10.1021/ja404580r.

Hydrogen Activation by Biomimetic [NiFe]-Hydrogenase Model Containing Protected Cyanide Cofactors

Brian C. Manor and **Thomas B. Rauchfuss***
School of Chemical Sciences, University of Illinois Urbana, IL 61801

Abstract

Described are experiments that allow incorporation of cyanide cofactors and hydride substrate into active site models [NiFe]-hydrogenases (H_2ases). Complexes of the type $(CO)_2(CN)_2Fe(pdt)Ni(dxpe)$, (dxpe = dppe, **1**; dxpe = dcpe, **2**) bind the Lewis acid $B(C_6F_5)_3$ (BAr^F_3) to give the adducts $(CO)_2(CNBAr^F_3)_2Fe(pdt)Ni(dxpe)$, (**1**$(BAr^F_3)_2$, **2**$(BAr^F_3)_2$). Upon decarbonylation using amine oxides, these adducts react with H_2 to give hydrido derivatives $Et_4N[(CO)(CNBAr^F_3)_2Fe(H)(pdt)Ni(dxpe)]$, (dxpe = dppe, $Et_4N[H$**3**$(BAr^F_3)_2]$; dxpe = dcpe, $Et_4N[H$**4**$(BAr^F_3)_2]$). Crystallographic analysis shows that $Et_4N[H$**3**$(BAr^F_3)_2]$ generally resembles the active site of the enzyme in the reduced, hydride-containing states (Ni-C/R). The Fe-H···Ni center is unsymmetrical with $r_{Fe\text{-}H}$ = 1.51(3) and $r_{Ni\text{-}H}$ = 1.71(3) Å. Both crystallographic and ^{19}F NMR analysis show that the $CNBAr^F_3{}^-$ ligands occupy basal and apical sites. Unlike cationic Ni-Fe hydrides, $[H$**3**$(BAr^F_3)_2]^-$ and $[H$**4**$(BAr^F_3)_2]^-$ oxidize at mild potentials, near the $Fc^{+/0}$ couple. Electrochemical measurements indicate that in the presence of base, $[H$**3**$(BAr^F_3)_2]^-$ catalyzes the oxidation of H_2. NMR evidence indicates dihydrogen bonding between these anionic hydrides and ammonium salts, which is relevant to the mechanism of hydrogenogenesis. In the case of $Et_4N[H$**3**$(BAr^F_3)_2]$, strong acids such as HCl induce H_2 release to give the chloride $Et_4N[(CO)(CNBAr^F_3)_2Fe(pdt)(Cl)Ni(dppe)]$.

Introduction

The hydrogenases (H_2ases) are represented by three main families of enzymes defined by the metals at their active sites, the [FeFe]-, [Fe]-, and [NiFe]-H_2ases.[1] Other enzymes consume or produce hydrogen,[2] but the [FeFe] and [NiFe]-H_2ases are renown for their ability to catalyze the oxidation of H_2 and reduction of protons at high rates and low overpotentials.[3]

The active sites of the hydrogenases are characterized by the presence of several remarkable cofactors. Crystallographic and spectroscopic analyses consistently point to the presence of $Fe(CO)_x(CN)_y$ sites in both types of redox active hydrogenases.[4] The diatomic cofactors are unusual in biology.[5] As indicated by close contacts between otherwise nonbonded heteroatoms, the Fe-C*N* centers anchor the active sites to the protein by means of hydrogen bonding. For example in the [NiFe]-H_2ase from *D. fructosovorans* one cyanide ligand hydrogen-bonds with serine 499 (N···N, N···O = 2.98, 2.88 Å, respectively). The second cyanide interacts with arginine 476, with N···N distances of 2.87 and 3.25 Å.[6] Some of

*Corresponding Author rauchfuz@illinois.edu.

Supporting Information ^1H NMR, ^{19}F NMR, ^{31}P NMR, and IR spectra for new compounds. CIF files giving X-ray crystallographic data. This material is available free of charge via the Internet at http://pubs.acs.org.

Notes The authors declare no competing financial interest.

these amino acids can be mutated with retention of catalytic activity,[7] which suggests that the N-terminus of the cyanide cofactors could be modified in models as well.

Motivated both by the novelty of the active site as well as possible practical applications, much effort has been invested into the structural and functional models of the [NiFe]-H_2ase active site.[1,8] Since 2009, several nickel-iron hydrides have been reported, but all of these models feature $Fe(CO)_{3-x}(PR_3)_x$ centers (x = 0, 1, 2).[9-12] In contrast to these cationic models, the active site is expected to be anionic since six cofactors - two cyanide and four thiolate groups - are anionic.[13] Incorporation of cyanide cofactors in models is avoided because the reactivity of the basic nitrogen site of cyanide.[14] Structural modes for a CO-inhibited state of the [NiFe]-H_2ases with cyanide cofactors have been reported, $(CN)_2(CO)_2Fe(SR)_2Ni(dppe)$ (**1**) (dppe = $(C_2H_4(PPh_2)_2)$[15] and $[(CN)_2(CO)_2Fe(SR)_2Ni(S_2CNEt_2)]^-$.[16] Both complexes feature $Fe(CO)_2(CN)_2$ centers bound to $Ni(SR)_2L_2$ sites. These complexes exhibit no biomimetic reactivity because of the coordinatively saturated nature of the $Fe(CN)_2(CO)_2(SR)_2$ sites.

This paper describes a method for modifying Fe-C*N* centers to suppress their high basicity[14] but retain the charge provided by the anionic cofactors. The approach entails attaching organoboranes to the Fe-C*N* groups. Although novel for metallobiochemistry, the interaction of boranes with metal cyanides is well known[17] and is exploited in commercial hydrocyanation catalysis.[18]

In view of the inertness of cyanide-containing models for the [NiFe]-H_2ases, attachment boranes to the Fe-C*N* centers could both labilize one CO ligand and suppress reactions of the Fe-C*N* centers, giving rise to reactive Ni^{II}-Fe^{II} centers capable of capturing a hydride substrate from dihydrogen.

Results and Discussion

N-Protected Active Site Models

Modeling efforts focused on the dicyano Ni-Fe dithiolate **1**, which was prepared by combining $NiCl_2(dppe)$ and $[Fe(CN)_2(pdt)(CO)_2]^{2-}$. Initial efforts to induce reactivity reminiscent of the H_2ases focused on the decarbonylation of this species. The FT-IR spectrum of **1** exhibits a relatively high frequency ν_{CO} band at 2053 cm^{-1}, suggesting that CO would be labile. UV-irradiation of a THF solution of **1** however afforded only insoluble solids, which are tentatively attributed to the formation of Fe-CN-M (M = Fe, Ni) linkages. Solutions of **1** were also found to be inert towards the decarbonylating agent Me_3NO.

Next examined was the use of boranes to protect the Fe-C*N* centers while also electrophilically activating the iron center. A variety of triarylboranes were found to form adducts with **1**, but this work focuses on $B(C_6F_5)_3$ (BAr^F_3). Adducts of this strong Lewis acid are often highly soluble in nonpolar solvents compatible with H_2 activation experiments.[19] Treatment of CH_2Cl_2 solutions of **1** with two equiv of BAr^F_3 quantitatively afforded the 2:1 adduct $(CO)_2(CNBAr^F_3)_2Fe(pdt)Ni(dppe)$, **1**$(BAr^F_3)_2$ (eq 1). The attachment of BAr^F_3 strongly affects the ν_{CN} and ν_{CO} bands, resulting in shifts of about 100 and 50 cm^{-1}, respectively (Table S1). The pattern of the $\nu_{CO/CN}$ bands is similar for the precursor and the adduct, consistent with retention of the cis-CO/trans-CN arrangement. ^{31}P and ^{19}F NMR spectra are also consistent with the proposed stereochemistry.

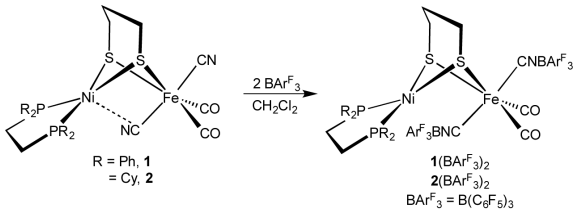

The structure of **1**$(BAr^F_3)_2$ was verified by X-ray crystallography (Fig. 2). Owing to the steric bulk of the BAr^F_3 groups, the Ni-Fe distance increased from 2.809 in **1** to 3.218 Å in the adduct.[15] Similarly the Ni-S-Fe angles opened from 75.98 to 86.60°. The BAr^F_3 substituents only subtly affect the diatomic ligands: the Fe-CN bonds are slightly elongated (Δ_{avg} = 0.03 Å) and the Fe-CO bond is slightly shortened (Δ_{avg} = −0.03 Å). The weak Ni···CN π-interaction (2.421 Å) apparent in **1**[15] is absent in **1**$(BAr^F_3)_2$.

To examine the effects of the basicity of nickel, $(CO)_2(CN)_2$Fe(pdt)Ni(dcpe) (**2**), featuring the highly basic ligand dcpe ($C_2H_4(P(C_6H_{11})_2)_2$), was also investigated. IR and ^{31}P NMR spectroscopy shows that **2** exists as a mixture of isomers, consisting of both the cis-CO/trans-CN arrangement (as seen in **1**) and the cis-CO/cis-CN arrangement. The decreased Lewis acidity of the Ni(dcpe) center, associated with the strong donor properties of dcpe,[20] is proposed to weaken the Ni-*NC*Fe interaction, giving rise to the second isomer. Much like **1**, **2** was found to be unreactive toward Me_3NO and decomposed in ambient light. Complexation of **2** with BAr^F_3 gave a pair of isomeric adducts of the formula $(CO)_2(CNBAr^F_3)_2$Fe(pdt)Ni(dcpe), **2**$(BAr^F_3)_2$. Over the course of several hours, this mixture converted to the cis-CO/trans-CN arrangement seen for **1**$(BAr^F_3)_2$.

The attachment of BAr^F_3 to the cyanide ligands stabilizes isomers not observed in **1** and **2**. As determined by ^{19}F and ^{31}P NMR spectroscopy, the cis-CO/trans-CN isomer of **1**$(BAr^F_3)_2$ converted to the cis-CO/cis-CN isomer upon heating at 60 °C. Upon UV-irradiation (365 nm), **1**$(BAr^F_3)_2$ converted to the trans-CO/cis-CN isomer as well as a small amount of the cis-CO/cis-CN isomer. Upon standing, trans-CO/cis-CN reverted to one of the two cis/cis isomers. Irradiation of the latter regenerated the trans-CO/cis-CN isomer (eq 2, showing only one of two cis/cis isomers). In no case was the cis-CO/trans-CN isomer of **1**$(BAr^F_3)_2$ observed to reform, which is apparently a kinetically stabilized isomer.

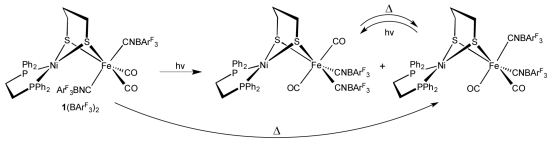

Irradiation of the cis-CO/trans-CN isomer of **2**$(BAr^F_3)_2$ gave the trans-CO/cis-CN isomer. Unlike in **1**$(BAr^F_3)_2$, the cis-CO/cis-CN isomer of **2**$(BAr^F_3)_2$ was not found to reform. Iron carbonyl complexes with high frequency ν_{CO} bands are typically photolabile. Indeed photolysis of cis-CO/trans-CN **1**$(BAr^F_3)_2$ under an atmosphere of ^{13}CO gave complete exchange of CO while forming the trans-CO/cis-CN isomer. Furthermore, the photoisomerization of **1**$(BAr^F_3)_2$ was found to be inhibited by CO. These results are consistent with a dissociative pathway for the photoisomerization of **1**$(BAr^F_3)_2$ and **2**$(BAr^F_3)_2$.

Hydride Derivatives

Being coordinatively saturated, the adducts **1**$(BAr^F{}_3)_2$ and **2**$(BAr^F{}_3)_2$ are unreactive toward H_2. Addition of a decarbonylation agent, however, was found to induce rapid uptake of hydrogen (eq 3).

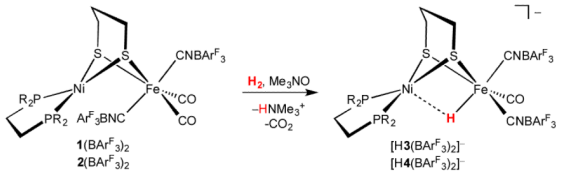

Thus, treatment of a CH_2Cl_2 solution of **1**$(BAr^F{}_3)_2$ with 1.2 equiv of an amine oxide under an atmosphere of H_2 afforded the hydride $[(CO)(CNBAr^F{}_3)_2Fe(pdt)(H)Ni(dppe)]^-$, which was isolated as the salt $Et_4N[H\mathbf{3}(BAr^F{}_3)_2]$. The use of D_2 in place of H_2 gave $Et_4N[D\mathbf{3}(BAr^F{}_3)_2]$, as verified by ^1H and ^2H NMR analyses. The decarbonylation agent Me_3NO gave an initial mixture of isomers with the $CNBAr^F{}_3$ ligands in dibasal (b/b) and apical-basel (a/b) arrangement in a 1:9.5 ratio. Upon standing in solution, the b/b isomer converted solely to the a/b isomer. Decarbonylation of **1**$(BAr^F{}_3)_2$ with N-methylmorpholine-N-oxide (NMO) produced the b/b isomer as the major species (2.5:1 b/b:a/b ratio). Similarly, decarbonylation of **2**$(BAr^F{}_3)_2$ under H_2 produced the a/b isomer of $Et_4N[(CO)(CNBAr^F{}_3)_2Fe(H)(pdt)Ni(dcpe)]$ ($Et_4N[H\mathbf{4}(BAr^F{}_3)_2]$) when Me_3NO was used as a decarbonylating agent with no b/b isomer observed.

The hydrides $[H\mathbf{3}(BAr^F{}_3)_2]^-$ and $[H\mathbf{4}(BAr^F{}_3)_2]^-$ were also produced using conventional hydride sources instead of H_2. Thus, treatment of $[\mathbf{1}(BAr^F{}_3)_2]$ with amine oxides followed by Et_4NBH_4 gave $Et_4N[H\mathbf{3}(BAr^F{}_3)_2]$. However, attempted synthesis of $Et_4N[H\mathbf{4}(BAr^F{}_3)_2]$ by treatment of **2**$(BAr^F{}_3)_2$ with amine oxides and Et_4NBH_4 produced more complicated results, yielding both monocarbonyl and dicarbonyl hydrides. Overall, H_2 is a gentler, more selective reagent for generating hydrido complexes.

As observed in the enzymes, the IR spectra of $[H\mathbf{3}(BAr^F{}_3)_2]-$ and $[H\mathbf{4}(BAr^F{}_3)_2]-$ display two ν_{CN} and one ν_{CO} bands. The energy for ν_{CO} of $[H\mathbf{4}(BAr^F{}_3)_2]-$ is 11 cm^{-1} lower than that of $[H\mathbf{3}(BAr^F{}_3)_2]-$ indicating that changes at the Ni center (dppe vs dcpe) influences the Fe site. Values of ν_{CO} for $[H\mathbf{3}(BAr^F{}_3)_2]-$ and $[H\mathbf{4}(BAr^F{}_3)_2]-$ were found to be within the range observed for the Ni-R state of [NiFe]-H_2ase (Table 1).

Structure of $Et_4N[H3(BAr^F{}_3)_2]$ and Comparisons with Enzyme Active Site

The structure of $[H\mathbf{3}(BAr^F{}_3)_2]^-$ was confirmed by single crystal X-ray diffraction (Fig. 3). The hydride of $[H\mathbf{3}(BAr^F{}_3)_2]^-$ was located in the difference Fourier map and refined isotropically. The Fe-H distance of 1.51(3) Å is shorter than the Ni-H bond (1.71(3) Å). In several respects, the structure of $[H\mathbf{3}(BAr^F{}_3)_2]^-$ resembles the high resolution (1.4, 1.5 Å) structures of the hydride-containing states (Ni-C/R) of *D. vulgaris* (Table 2).[22] The Fe···Ni distance of 2.5497(5) Å reasonably matches the values 2.59 and 2.57 Å found in these hydride-containing states. Reminiscent of the active site, the coordination geometry of the NiS_2P_2 center is distorted from square planar, with a twist angle between the NiS_2 plane and NiP_2 plane of 34.53°. Like the enzyme, iron is bound to one CO and two CN-derived ligands although the locations of the CO and the one $CNBAr^F{}_3{}^-$ are interchanged relative to the enzyme.

Reactivity of the Hydrido Complexes

The redox properties of [H**3**$(BAr^F{}_3)_2]^-$ and [H**4**$(BAr^F{}_3)_2]^-$ were assessed by cyclic voltammetry on CH_2Cl_2 solutions. These results underscore the influence of anionic donor ligands on the Fe site. Both hydrides oxidize at mild potentials: −0.08 V vs $Fc^{0/+}$ (i_{pc}/i_{pa} = 0.43, scan rate = 0.1 V/s) for Et_4N[H**3**$(BAr^F{}_3)_2]$ and −0.10 V (i_{pc}/i_{pa} = 0.69, scan rate = 0.1 V/s) for Et_4N[H**4**$(BAr^F{}_3)_2]$ (Figs. S29, S30). The insensitivity of the [H**3**$(BAr^F{}_3)_2]^{-/0}$ vs [H**4**$(BAr^F{}_3)_2]^{-/0}$ couples to the diphosphine suggests that oxidation is localized on Fe. In the enzyme, oxidation of the Ni-R state is localized on Ni.

Reflecting their anionic character, both complexes reduce at more negative potentials in comparison with previously reported NiFe hydrides. A reversible reduction was observed for Et_4N[H**3**$(BAr^F{}_3)_2]$ at −1.99 V (Fig. S28) but no reduction was observed for Et_4N[H**4**$(BAr^F{}_3)_2]$ within the potential window of CH_2Cl_2 (< −2.5 V). Cationic NiFe hydrides, i.e., those based on $Fe(CO)_{3-x}(PR_3)_x$ centers, reduce at milder potentials (−1.33 to −1.56 V vs $Fc^{0/+}$).[10,11] Reduction potentials for those cationic Fe(II)Ni(II) hydrides are sensitive to substitution at Ni (dppe vs dcpe) and Fe (CO vs PR_3).[10,11]

The acid base properties of [H**3**$(BAr^F{}_3)_2]^-$ and [H**4**$(BAr^F{}_3)_2]^-$ were examined, with limited success. Unlike cationic Ni-Fe hydrides, which exhibit pK_a^{MeCN} near 14, CH_2Cl_2 solution of [H**3**$(BAr^F{}_3)_2]^-$ did not undergo deprotonation upon treatment with the strong base DBU (pK_a^{MeCN} = 24.34). Solution of [H**3**$(BAr^F{}_3)_2]^-$ exhibit no exchange with D_2O.

Et_4N[H**3**$(BAr^F{}_3)_2]$ was found to be an electrocatalyst for the oxidation of H_2. When a solution was examined by cyclic voltammetry under 1 atm of H_2, the current at −0.08 V, corresponding to the [H**3**$(BAr^F{}_3)_2]^{-/0}$ couple, was found to increase upon addition of the base DBU (see Supporting Information).

Dihydrogen Bonding

The solution properties of [H**3**$(BAr^F{}_3)_2]^-$ are indicative of its hydridic character, consistent with its resemblance to the hydrogen-evolving state Ni-R. Specifically, the high field ^1H NMR signal of Et N[H**3**$(BAr^F$ 4 $3)_2]$ is sensitive to the presence of reagents that engage in dihydrogen bonding. For example, the addition of $HNMe_3[BAr^{F24}]$ (pK_a^{MeCN} = 17.61)[23] shifts the hydride signal (δ_H) by about 2 ppm (Figure 4). The dependence of δ_H on the concentration of $HNMe_3^+$ is consistent with an equilibrium constant of 9.0±1.0 × 10^3 L/mol in CD_2Cl_2 (20 °C, eq 3). Dihydrogen bonding is also evident in the ^1H NMR spectra when [H**4**$(BAr^F{}_3)_2]^-$ was titrated with [pyrrolidinium]BAr^{F24} (pK_a^{MeCN} = 19.56).[24] Although competitive with degradation of the complex, [H**3**$(BAr^F{}_3)_2]^-$ was found to undergo H/D scrambling with D_2, forming HD. This process occurs only in the presence of $HNMe_3^+$.

Although weak acids form dihydrogen bonds with [H**3**$(BAr^F{}_3)_2]^-$, stronger acids, $PhNH_3^+$ (pK_a = 10.62), induce release ~1 equiv of H_2. Using HCl, the unsaturated product is trapped as the chloride adduct [Cl**3**$(BAr^F{}_3)_2]^-$ (eq 4). The complex [Cl**3**$(BAr^F{}_3)_2]^-$ was independently prepared by the reaction of **1**$(BAr^F{}_3)_2$ with Me_3NO and Et_4NCl.

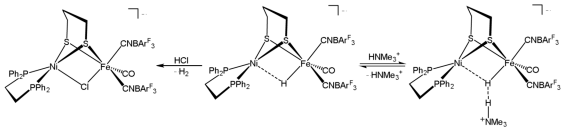

Conclusions

Borane protecting groups enable the preparation of the first models of the [NiFe]-H_2ases with biomimetic ligation at Fe. The protecting groups suppress reactions at the Fe-C*N* centers, while retaining the anionic charge that is characteristic of these active sites.

Similar to work with the enzyme,[21] models in this work were obtained in an inhibited state. Unlike the enzyme,[25] the CO-inhibited NiFe models contain an extra CO ligand on Fe.[26] Upon decarbonylation, the borane-protected Ni-Fe derivatives abstract hydride from H_2. The generation of hydrides from H_2 is unusual in H_2ase models[12,27] but is a key reaction of the enzyme. On the basis of structural and ν_{CO} data, these models compare well with the Ni-R state.[28]

The redox properties of the hydrides [H**3**$(BAr^F{}_3)_2]^-$ and [H**4**$(BAr^F{}_3)_2)]^-$ provide insights into the design of improved active site models. Because the basicities of dppe and dcpe differ greatly[20] and the oxidations potentials differ by only 20 mV, these oxidations are assigned to the $Fe^{II/III}$ couple. In contrast, oxidation of the Ni-R state to the Ni-C state is localized on nickel, i.e., a Ni^{II}-Fe^{II}/Ni^{III}-Fe^{II} couple.[29] These findings point to the limitations of diphosphines as mimics for the terminal ligands on the Ni site. As suggested with a recent model,[30] the terminal thiolate ligands in the enzyme[1] change their protonation state upon redox of the Ni center. Future models could benefit by including terminal ligands that have ionizable protons such as RS*H*.

Compared to cationic nickel-iron hydrides,[10-12] the anionic models exhibit more biomimetic electrochemical and acid-base properties. Most importantly, anionic nickel-iron hydrides have hydridic character[31] as indicated by NMR studies showing dihydrogen bonding, which leads to hydrogen evolution. On the basis of these results, a similar dihydrogen bond in the Ni-R state is proposed to precede H_2 evolution (Figure 5).

Bridging hydrides in related systems have protic character and do not engage in dihydrogen bonding.[32] Dihydrogen bonding involving terminal iron hydrides is observed in models for the active site of the [FeFe]-H_2ases.[33] Thus it appears that the hydrides of [FeFe]- and [NiFe]-H_2ases (in the Ni-R state) are similar in being hydridic.

Experimental Section

All procedures were carried out in a nitrogen filled MBraun glovebox or using standard Schlenk techniques. All solvents were degassed by sparging with nitrogen and dried by passage through activated alumina. IR spectra were recorded on a Perkin Elmer Spectrum 100. Cyclic voltammetry was performed under argon at room temperature using a CHI 630D potentiostat with glassy carbon working electrode, Pt wire counter electrode and the pseudo-reference electrode Ag wire, and with Fc internal standard. Production of H_2 was quantified by gas chromatography on a column packed with 5 Å molecular sieves (carrier gas: Ar), using an Agilent 7820A instrument equipped with a thermal conductivity detector. The response factor for H_2/CH_4 was 3.8 under experimental conditions as established by calibration with standard H_2-CH_4 mixtures. NMR spectra were recorded on a Varian Unity 500 MHz NMR spectrometer. Signals for ^{19}F and ^{31}P NMR spectra were referenced using external standards of 1%$CFCl_3$ in $CDCl_3$ and 85% H_3PO_4, respectively. ^1H NMR spectra were referenced to internal solvent signals. CD_2Cl_2 (Cambridge Isotope Laboratories) was dried over CaH_2 before being vacuum distilled onto activated 4Å molecular sieves. $B(C_6F_5)_3$ (Boulder Scientific) was sublimed under vacuum at 90 °C. Literature routes were followed for $NiCl_2$(dppe),[9] $NiCl_2$(dcpe),[11] $Et_4N[Fe(CO)_4(CN)]$,[34] K_2pdt,[16] and $Et_4N[FeBr(CO)_3(CN)_2]$.[16]

Revised Synthesis of $(CO)_2(CN)_2Fe(pdt)Ni(dppe)$, 1

A solution of $Et_4N[FeBr(CO)_3(CN)_2]$ (0.900 g, 2.22 mmol) in MeOH (100 mL) was treated with a solution of K_2pdt (0.410 g, 2.22 mmol) in MeOH (50 mL). The mixture was allowed to stir for 3 h at which time the solvent was removed under vacuum. $NiCl_2(dppe)$ (1.17 g, 2.22 mmol) was added along with 100 mL of MeCN and the mixture was stirred for 15 min. The mixture was filtered, and the solvent was removed from the filtrate under vacuum. The crude product was extracted into THF, and the crude product was precipitated from the filtered extract upon the addition of pentane. The crude product was dissolved in MeCN and loaded onto a neutral alumina column (Brockmann Level I). A faint red band was washed off the column with MeCN. The product eluted with MeOH as a red band. The solution was evaporated under vacuum, and the residue was extracted into THF. This solution was filtered through Celite, and product was precipitated from the filtrate with pentane. The product[16] was collected by filtration and dried under vacuum. Yield: 0.958 g (59%).

$(CO)_2(CN)_2Fe(pdt)Ni(dcpe)$, 2

A solution of $Et_4N[FeBr(CO)_3(CN)_2]$ (0.500 g, 1.23 mmol) in MeOH (20 mL) was treated with a solution of K_2pdt (0.228 g, 1.23 mmol) in MeOH (20 mL). The mixture was let to stir for 3 h at which time the solvent was removed under vacuum. In the absence of light, the residue was extracted into 20 mL of MeCN, and the mixture was treated with a suspension of $NiCl_2(dcpe)$ (0.682 g, 1.23 mmol) in MeCN (20 mL). After stirring for 15 min, the mixture was filtered and the solvent was stripped from the filtrate. The crude product was extracted into 20 mL of THF, the mixture was filtered, and the product was precipitated from the filtrate upon the addition of pentane. Unlike **1**, **2** did not require further purification by column chromatography. Yield: 0.423 g (45%). Anal. Calcd for $C_{33}H_{54}FeN_2NiO_2P_2S_2$ (found): C, 52.75 (52.34); H, 7.24 (7.59); N, 3.73 (3.99).

Data for cis-CO/trans-CN isomer: IR(CH_2Cl_2, cm^{-1}): ν_{CN} = 2113, 2090; ν_{CO} = 2045, 1995. ^{31}P NMR (CD_2Cl_2): δ 66.3 (s).

Dats for cis-CO/cis-CN isomer: IR (CH_2Cl_2, cm^{-1}): ν_{CN} = 2120, ν_{CO} = 2033, 1982. ^{31}P NMR (CD_2Cl_2): δ 67.8, 66.5 (AB quartet, J_{pp} = 33 Hz).

$(CO)_2(CNBAr^F{}_3)_2Fe(pdt)Ni(dppe)$, $1(BAr^F{}_3)_2$

A solution of $(CO)_2(CN)_2Fe(pdt)Ni(dppe)$ (290 mg, 0.4 mmol) in 10 mL of CH_2Cl_2 was treated with a solution of $BAr^F{}_3$ (410 mg, 0.8 mmol) in 30 mL of CH_2Cl_2 dropwise. The reaction caused a change in color from a red to an orange solution. The reaction solution was concentrated to 20 mL and layered with 100 mL of pentane followed by cooling to −30 °C. Yield: 570 mg (82%). Crystals suitable for X-ray diffraction were grown from a concentrated THF solution of $\mathbf{1}(BAr^F{}_3)_2$ layered with pentane and cooled at −30°C. IR (CH_2Cl_2, cm^{-1}): ν_{CN} = 2194, 2166, ν_{CO} = 2088, 2050. ^{31}P NMR (CD_2Cl_2): δ 56.4 (s). ^{19}F NMR (CD_2Cl_2): δ −133.7 (d, *o*-F) −135.1 (d, *o*-F), −159.2 (t, *p*-F) −159.4 (t, *p*-F), −165.0 (dt, *m*-F) −165.6 (dt, *m*-F). Anal. Calcd for $C_{69}H_{30}B_2F_{30}FeN_2NiO_2P_2S_2$ (found): C, 47.32 (47.24); H, 1.73 (1.64); N, 1.60 (1.52).

$(CO)_2(CNBAr^F{}_3)_2Fe(pdt)Ni(dcpe)$, $2(BAr^F{}_3)_2$

Analogously to the preparation of $1(BAr^F{}_3)_2$, a solution of 2 (0.144 g, 0.0192 mmol) in CH_2Cl_2 (5 mL) was treated with a solution of $BAr^F{}_3$ (0.196 g, 0.0383 mmol) resulting in a color change from red or orange. The solvent was removed under vacuum, redissolved in THF and crystallized by the addition of pentane followed by cooling to −30 °C. Yield: 0.253 g (74%).

Data for cis-CO/trans-CN isomer: IR (CH_2Cl_2, cm^{-1}): ν_{CN} = 2190, 2149, ν_{CO} = 2085, 2046. ^{31}P NMR (CD_2Cl_2): δ 69.8 (s). ^{19}F NMR (CD_2Cl_2): −133.8 (d, o-F), −134.2 (d, o-F), −159.4 (t, p-F), −160.6 (t, p-F), −165.3 (t, m-F), −166.4 (t, m-F).

Data for cis-CO/cis-CN isomer: IR (CH_2Cl_2, cm^{-1}): ν_{CN} = 2210; ν_{CO} = 2068, 2030. ^{31}P NMR (CD_2Cl_2): δ 70.2, 69.5 (AB quartet, J_{PP} = 30 Hz). ^{19}F NMR (CD_2Cl_2): −133.1 (d, *o*-F), −134.9 (o-F), −158.7 (t, *p*-F), −159.3 (t, *p*-F), −165.0 (t, *m*-F), −165.5 (t, *m*-F).

$Et_4N[(CO)(CNBAr^F{}_3)_2Fe(pdt)(H)Ni(dppe)]$, $Et_4N[H3(BAr^F{}_3)_2]$

In a thick-walled glass pressure tube, a solution of **1**$(BAr^F{}_3)_2$ (150 mg, 0.0857 mmol) in CH_2Cl_2 (10 mL) was frozen by inserting the tube into liquid nitrogen. Under a flow of Ar, a buffer layer of CH_2Cl (5 mL) was frozen on top of the frozen solution of **1**$(BAr^F{}_3)_2$. A solution of Me_3NO (7.7 mg, 0.103 mmol) in CH_2Cl_2 (2 mL) was frozen on top of the buffer layer. The head space was evacuated and refilled with 40 psig of H_2 followed by thawing of the frozen solution. After stirring the mixture for 2 h, the solvent was removed under vacuum, and the residue was extracted into Et_2O. The extract was filtered through Celite and analyzed by ^{19}F NMR spectroscopy, which showed 60% of signals corresponded to product. A solution of this sample in 10 mL of CH_2Cl_2 was stirred with excess Et_4NCl (142 mg, 0.857 mmol). The solvent was removed under vacuum, and the product was extracted into 10 mL of THF, which was then filtered through Celite and evaporated. The solid was dissolved in a minimal amount of THF and loaded onto a column of neutral alumina (Brockmann Level IV) packed with THF. A red band eluted with THF and was discarded. The remaining brown band was eluted off the column using CH_2Cl_2. The solution was concentrated to 5 mL, layered with 20 mL of pentane, and cooled to −30 °C yielding red crystals (44 mg, 28%). IR (CH_2Cl_2, cm^{-1}): ν_{CN} = 2162, 2137, ν_{CO} = 1963. ^1H NMR (CD_2Cl_2): δ −7.05 (t, J_{HP} = 5.2 Hz). $^{31}P\{^1H\}$ NMR (CD_2Cl_2): δ −66.6 (s). ^{19}F NMR (CD_2Cl_2): δ −134.4 (*o*–F), −162.5 −162.9 (t, *p*–F), −167.4 −167.6 (t, *m*–F). Anal. Calcd for $C_{76}H_{51}B_2F_{30}FeN_3NiOP_2S_2 \cdot 0.3CH_2Cl_2$ (found): C, 48.83 (48.81); H, 2.77 (2.43); N, 2.30 (2.24). Use of N-methylmorpholine-N-oxide in place of Me_3NO favored the b/b isomer. $Et_4N[H\mathbf{3}(BAr^F{}_3)_2]$ was prepared from **1**$(BAr^F{}_3)_2$ and Me_3NO using Et_4NBH_4 as the hydride source (see SI).

$Et_4N[(CO)(CNBAr^F{}_3)_2Fe(pdt)(H)Ni(dcpe)]$, $Et_4N[H4(BAr^F{}_3)_2]$

This compound was prepared in a manner and yield similar to the preparation of $Et_4N[H\mathbf{3}(BAr^F{}_3)_2]$. IR ($CH_2Cl_2$, cm^{-1}): ν_{CN} = 2158, 2132; ν_{CO} = 1952. ^1H NMR (CD_2Cl_2): δ −6.56 (t, J_{HP} = 3 Hz). $^{31}P\{^1H\}$ NMR (CD_2Cl_2): δ −85.1 (s). ^{19}F NMR (CD_2Cl_2): δ −134.3 (d, *o*–F), −162.5 −163.0 (t, *p*–F), −167.3 −167.8 (t, *m*–F). Anal. Calcd for $C_{76}H_{75}B_2F_{30}FeN_3NiOP_2S_2$ (found): C, 48.58 (48.83); H, 4.02 (4.00); N, 2.24 (2.35).

$Et_4N[(CO)(CNBAr^F{}_3)_2Fe(pdt)(Cl)Ni(dppe)]$, $Et_4N[Cl3(BAr^F{}_3)_2]$

A solution of $Et_4N[H\mathbf{3}(BAr^F{}_3)_2]$ (10 mg, 0.0054 mmol) in CD_2Cl_2 (0.7 mL) was treated with HCl (2M in Et_2O, 6 μL, 2.2 equiv, 0.012 mmol) resulting the solution turning slightly lighter in color. ^1H NMR confirmed the formation of H_2. ^{31}P NMR displayed a major species (~60%) as an AB quartet at δ–51.5 and −48.6 and ^{19}F NMR displayed signals for two inequivalent $BAr^F{}_3$ environments, both consistent with an apical/basal arrangement of $CNBAr^F{}_3{}^-$ ligands. Assignment of this major species as $Et_4N[Cl\mathbf{3}(BAr^F{}_3)_2]$ was confirmed by independent synthesis of $Et_4N[Cl\mathbf{3}(BAr^F{}_3)_2]$ from **1**$(BAr^F{}_3)_2$ and Et_4NCl. Thus, a solution of **1**$(BAr^F{}_3)_2$ (0.10 g, 0.057 mmol) in CH_2Cl_2 (10 mL) was treated with a solution of Me_3NO (5.1 mg, 0.069 mmol) in CH_2Cl_2 (1 mL) followed by Et_4NCl (9.5 mg, 0.057 mmol) in CH_2Cl_2 (5 mL). After the solution was allowed to stir for 15 min., solvent was removed under vacuum. The crude solid was dissolved in a minimal amount of THF and loaded onto a column of neutral alumina (Brockmann Level IV) eluting THF. The first red

band was discarded, and the remaining brown band was eluted with CH_2Cl_2. The solution was concentrated to 5 mL, layered with 20 mL of pentane, and cooled to −30 °C precipitating an oil. Upon storing under vacuum, the oil converted to a solid (40 mg, 37%). IR (CH_2Cl_2, cm^{-1}): ν_{CN} = 2181, 2149; ν_{CO} = 1996. $^{31}P\{^1H\}$ NMR (CD_2Cl_2): δ −51.5, −48.6 (AB quartet, J_{PP} = 29 Hz). ^{19}F NMR (CD_2Cl_2): δ −134.1, −134.6 (d, *o*–F); −161.9, −162.4 (t, *p*–F); −167.0, −167.2 (t, *m*–F). Anal. Calcd for $C_{76}H_{50}B_2ClF_{30}FeN_3NiOP_2S_2$ (found): C, 48.33 (48.30); H, 2.67 (2.43); N, 2.22 (2.43).

Supplementary Material

Refer to Web version on PubMed Central for supplementary material.

Acknowledgments

This research was supported by NIH and the International Institute for Carbon Neutral Energy Research (WPI-I2CNER), sponsored by the World Premier International Research Center Initiative (WPI), MEXT, Japan. We thank Danielle Gray for assistance with the crystallography and Prof. Steven Zimmerman and Ying Li for assistance with the calculations of the binding constants.

REFERENCES

(1). Tard C, Pickett CJ. Chem. Rev. 2009; 109:2245. [PubMed: 19438209]

(2). Fontecilla-Camps JC, Amara P, Cavazza C, Nicolet Y, Volbeda A. Nature. 2009; 460:814. [PubMed: 19675641]

(3). Fontecilla-Camps JC, Volbeda A, Cavazza C, Nicolet Y. Chem. Rev. 2007; 107:4273. [PubMed: 17850165] Siegbahn PEM, Tye JW, Hall MB. Chem. Rev. 2007; 107:4414. [PubMed: 17927160] Vincent KA, Parkin A, Armstrong FA. Chem. Rev. 2007; 107:4366. [PubMed: 17845060]

(4). Ogata H, Lubitz W, Higuchi Y. Dalton Trans. 2009:7577. [PubMed: 19759926] Ogata H, Kellers P, Lubitz W. J. Mol. Biol. 2010; 402:428. [PubMed: 20673834]

(5). Böck A, King PW, Blokesch M, Posewitz MC. Adv. Microb. Physiol. 2006; 51:1. [PubMed: 17091562] Peters JW, Broderick JB. Annu. Rev. Biochem. 2012; 81:429. [PubMed: 22482905]

(6). Volbeda A, Martin L, Cavazza C, Matho M, Faber BW, Roseboom W, Albracht SPJ, Garcin E, Rousset M, Fontecilla-Camps JC. JBIC, J. Biol. Inorg. Chem. 2005; 10:239.

(7). De Lacey AL, Fernandez VM, Rousset M, Cavazza C, Hatchikian EC. J. Biol. Inorg. Chem. 2003; 8:129. [PubMed: 12459907]

(8). Ohki Y, Tatsumi K. Eur. J. Inorg. Chem. 2011; 2011:973.Gloaguen F, Rauchfuss TB. Chem. Soc. Rev. 2009; 38:100. [PubMed: 19088969]

(9). Barton BE, Whaley CM, Rauchfuss TB, Gray DL. J. Am. Chem. Soc. 2009; 131:6942. [PubMed: 19413314]

(10). Barton BE, Rauchfuss TB. J. Am. Chem. Soc. 2010; 132:14877. [PubMed: 20925337]

(11). Carroll ME, Barton BE, Gray DL, Mack AE, Rauchfuss TB. Inorg. Chem. 2011; 50:9554. [PubMed: 21866886]

(12). Ogo S, Ichikawa K, Kishima T, Matsumoto T, Nakai H, Kusaka K, Ohhara T. Science. 2013; 339:682. [PubMed: 23393260]

(13). Armstrong FA. Science. 2013; 339:658. [PubMed: 23393255]

(14). Jablonskyte A, Wright JA, Pickett CJ. Dalton Trans. 2010; 39:3026. [PubMed: 20221536]

(15). Jiang J, Maruani M, Solaimanzadeh J, Lo W, Koch SA, Millar M. Inorg. Chem. 2009; 48:6359. [PubMed: 20507106]

(16). Li Z, Ohki Y, Tatsumi K. J. Am. Chem. Soc. 2005; 127:8950. [PubMed: 15969562]

(17). Kristoff JS, Shriver DF. Inorg. Chem. 1973; 12:1788.Schelter EJ, Shatruk M, Heintz RA, Galan-Mascaros JR, Dunbar KR. Chem. Commun. 2005:1417.

(18). Brunkan NM, Brestensky DM, Jones WD. J. Am. Chem. Soc. 2004; 126:3627. [PubMed: 15025492]

(19). Stephan DW. Dalton Trans. 2009:3129. [PubMed: 19421613]

(20). Sowa JR Jr. Zanotti V, Facchin G, Angelici RJ. J. Am. Chem. Soc. 1992; 114:160.

(21). De Lacey AL, Fernández VM, Rousset M, Cammack R. Chem. Rev. 2007; 107:4304. [PubMed: 17715982]

(22). Ogata H, Hirota S, Nakahara A, Komori H, Shibata N, Kato T, Kano K, Higuchi Y. Structure. 2005; 13:1635. [PubMed: 16271886] Higuchi Y, Ogata H, Miki K, Yasuoka N, Yagi T. Structure. 1999; 7:549. [PubMed: 10378274]

(23). Coetzee JF, Padmanabhan GR. J. Am. Chem. Soc. 1965; 87:5005.

(24). Kaljurand I, Kütt A, Sooväli L, Rodima T, Mäemets V, Leito I, Koppel IA. J. Org. Chem. 2005; 70:1019. [PubMed: 15675863]

(25). Ogata H, Mizoguchi Y, Mizuno N, Miki K, Adachi S.-i. Yasuoka N, Yagi T, Yamauchi O, Hirota S, Higuchi Y. J. Am. Chem. Soc. 2002; 124:11628. [PubMed: 12296727]

(26). Ohki Y, Yasumura K, Ando M, Shimokata S, Tatsumi K. Proc. Natl. Acad. Sci. U. S. A. 2010; 107:3994. [PubMed: 20147622] Matsumoto T, Kabe R, Nonaka K, Ando T, Yoon K-S, Nakai H, Ogo S. Inorg. Chem. 2011; 50:8902. [PubMed: 21853978]

(27). Camara JM, Rauchfuss TB. Nature Chem. 2012; 4:26. [PubMed: 22169868]

(28). Fichtner C, Laurich C, Bothe E, Lubitz W. Biochemistry. 2006; 45:9706. [PubMed: 16893172]

(29). Lubitz W, Reijerse E, van Gastel M. Chem. Rev. 2007; 107:4331. [PubMed: 17845059]

(30). Weber K, Krämer T, Shafaat HS, Weyhermuller T, Bill E, van Gastel M, Neese F, Lubitz W. J. Am. Chem. Soc. 2012; 134:20745. [PubMed: 23194246]

(31). Raebiger JW, Miedaner A, Curtis CJ, Miller SM, Anderson OP, DuBois DL. J. Am. Chem. Soc. 2004; 126:5502. [PubMed: 15113222] Rakowski DuBois M, DuBois DL. Acc. Chem. Res. 2009; 42:1974. [PubMed: 19645445]

(32). Wang N, Wang M, Zhang T, Li P, Liu J, Sun L. Chem. Commun. 2008:5800.

(33). Carroll ME, Barton BE, Rauchfuss TB, Carroll PJ. J. Am. Chem. Soc. 2012; 134:18843. [PubMed: 23126330]

(34). Kayal A, Rauchfuss TB. Inorg. Chem. 2003; 42:5046. [PubMed: 12924874]

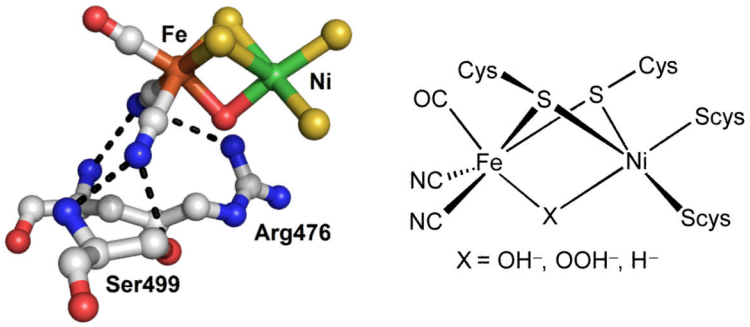

Figure 1.

Left: Active site of [NiFe]-H_2ase active site (Ni-B state) of *D. fructosovorans* with hydrogen-bonding interactions between Fe-CN and nearby residues (PDB 1YRQ). Right: Drawing of the active site of [NiFe]-H_2ase showing various bridging ligands.

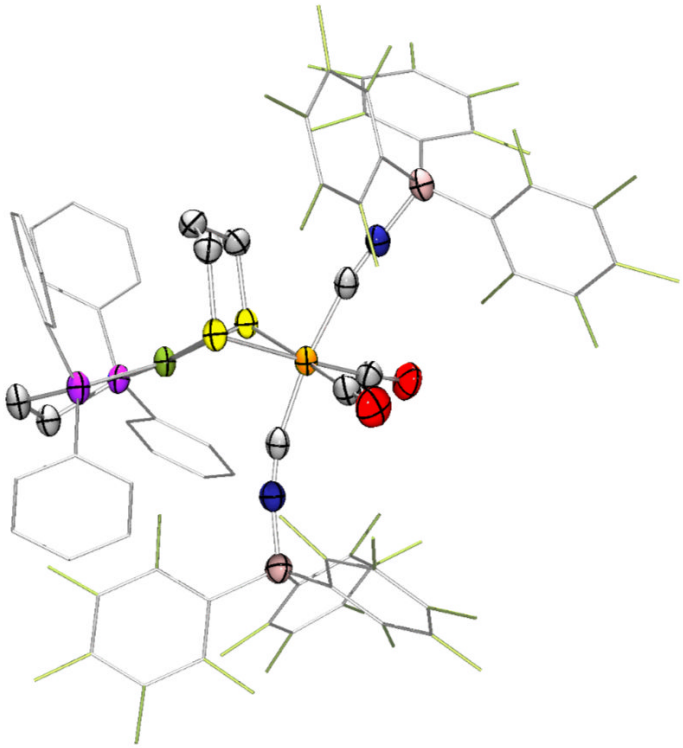

Figure 2.
Structure of $[(CO)_2(CNBAr^F{}_3)^2Fe(pdt)Ni(dppe)]$, **1**$(BAr^F{}_3)_2$ with ellipsoids shown at 50% probability and with H atoms omitted for clarity. Phenyl and pentafluorophenyl groups are deemphasized for clarity.

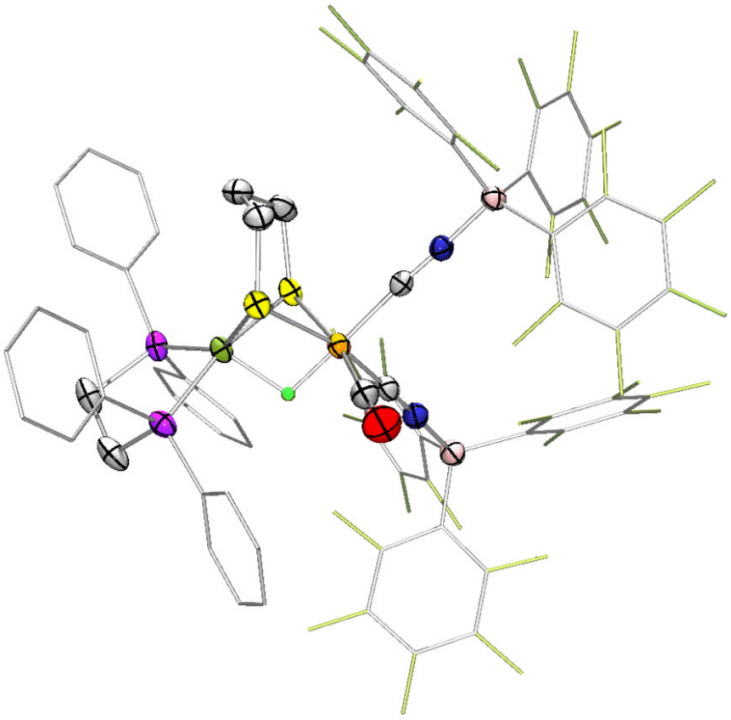

Figure 3.
Structure of the anion in $Et_4N[(CO)(CNBAr^F{}_3)_2Fe(pdt)(H)Ni(dppe)]$, $Et_4N[H\mathbf{3}(BAr^F{}_3)_2]$) with ellipsoids shown at 50% probability and H atoms except for the bridging hydride omitted. Phenyl and pentafluorophenyl groups are deemphasized for clarity.

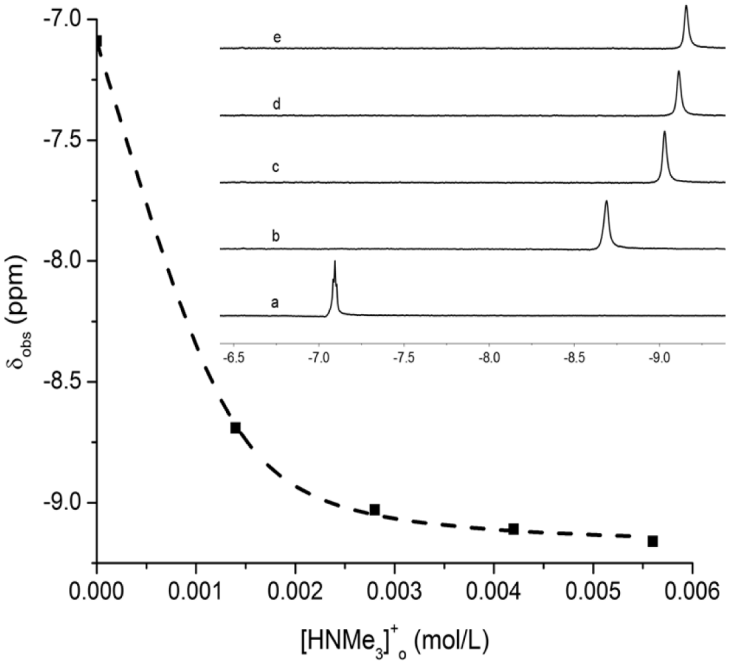

Figure 4.

^{1}H NMR chemical shift for $Et_4N[\mathit{H}\mathbf{3}(BAr^F{}_3)_2]$ upon titration with $HNMe_3[BAr^{F24}]$ in CD_2Cl_2 (20 °C). Inset: ^{1}H NMR (500 MHz) spectra of the titration of $Et_4N[H\mathbf{3}(BAr^F{}_3)_2]$ with $HNMe_3BAr^{F24}$ in CD_2Cl_2 (20 °C): a) 0, b) 1.0, c) 2.0, d) 3.0, and e) 4.0 equiv.

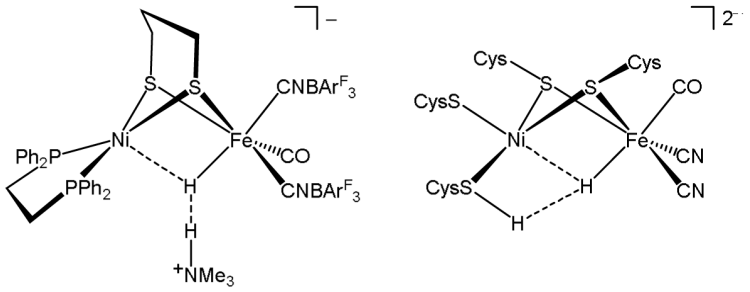

Figure 5.
Dihydrogen bonding in $[H\mathbf{3}(BAr^F{}_3)_2]^-$ and the analogous interaction proposed for Ni-R.

Table 1

IR Bands for the CN-protected Species [H**3**(BAr^F_3)$_2$]$^-$ and [H**4**(BAr^F_3)$_2$]$^-$ as well as [NiFe]-H_2ase Enzymes in the Ni-R State,[21] and Other Ni-R Models.[10]

Compound	ν_{CN} (cm^{-1})	ν_{CO} (cm^{-1})
Ni-R state, *A. vinosum*	2072, 2059	1936
Ni-R state, *D. gigas*	2073, 2060	1940
Ni-R state, *D. fructosovorans*	2074, 2060	1938
Ni-R state, *D. vulgaris*	2074, 2061	1948
[(CO)(CNBAr$^F_3$)$_2$Fe(H)(pdt)Ni(dppe)]$^-$([H**3**(BAr$^F_3$)$_2$]$^-$)	2162, 2137	1963
[(CO)(CNBAr$^F_3$)$_2$Fe(H)(pdt)Ni(dcpe)]$^-$ ([H**4**(BAr$^F_3$)$_2$]$^-$)	2158, 2131	1952
[(CO)$_2$(PPh$_3$)Fe(H)(pdt)Ni(dppe)]$^+$	-	2016, 1964

Table 2

Key Distances (Å) and Angles (°) of [H**3**(BAr^F_3)$_2$]$^-$ and the Active Site of *D. vulgaris* Miyazaki F in the Reduced State(s).[22]

	[(CO)(CNBAr$^F_3$)$_2$Fe(pdt)(H)Ni(dppe)]$^-$	***D. vulgaris* Miyazaki F Ni-C/R (PDB: 1H2R)**	***D. vulgaris* Miyazaki F Ni-C/R (PDB: 1WUL)**
Fe-Ni	2.5497(5)	2.59	2.57
Fe-H	1.51(3)	N/A	N/A
Ni-H	1.71(3)	N/A	N/A
Fe-C_{apical}	1.889(3) ($CNBAr^F_3{}^-$)	1.84 (CO)	1.80 (CO)
Fe-C_{basal}	1.758(3) (CO), 1.866(2) ($CNBAr^F_3{}^-$)	1.86 (CO), 2.21 (SO)	1.99 (CN^-), 2.03 (CO)
Fe-S	2.3246(6), 2.2977(8)	2.29, 2.36	2.26, 2.32
Ni-S	2.1952(8), 2.3046(8)	2.43, 2.33	2.23, 2.52
Ni-term-L	2.1382(8), 2.1591(8) (L = PR_3)	2.32, 2.24 (L =SR^-)	2.13, 2.21 (L = SR^-)
C_{basal}-Fe-C_{basal}	94.0(1)	89	93
C_{basal}-Fe-C_{apical}	90.6(1), 96.0(1)	90, 98	90, 95